SERBIAN JOURNAL OF ELECTRICAL ENGINEERING
Vol. 4, No. 1, June 2007, 51-69

Synchronous Machine Parameter Identification in Frequency and Time Domain

M. Hasni[1], S. Djema[1], O. Touhami[1], R. Ibtiouen[1], M. Fadel[2] and S. Caux[2]

Abstract: This paper presents the results of a frequency and time-domain identification procedure to estimate the linear parameters of a salient-pole synchronous machine at standstill. The objective of this study is to use several input signals to identify the model structure and parameters of a salient-pole synchronous machine from standstill test data. The procedure consists to define, to conduct the standstill tests and also to identify the model structure. The signals used for identification are the different excitation voltages at standstill and the flowing current in different windings.

We estimate the parameters of operational impedances, or in other words the reactance and the time constants.

The tests were carried out on synchronous machine of $1.5\,\mathrm{kVA}/380\,\mathrm{V}/1500\,\mathrm{rpm}$.

Keywords: Synchronous machine, Frequency tests, Standstill tests, DC-Chopper, PRBS (Pseudo Random Binary Sequences) voltages, PWM voltages and DC decay.

1 Introduction

The identification of synchronous machine parameters has been and still is an important topic of many publications. Different measurement techniques, identification procedures and models structures are developed to obtain models as accurate predictors for the transient behavior of generators [1-5].

Many papers have been published on synchronous machine modeling and parameter estimation using standstill frequency response data, standstill time response data, and rotating time domain response data and many propositions for the determination of synchronous machine parameters are suggested [1-6].

[1]Laboratoire de Recherche en Electrotechnique, Ecole Nationale Polytechnique, BP 182 El Harrach 16200, Algiers,Algeria,E-mail: hasnimourad2001@yahoo.fr, omar.touhami@enp.edu.dz, rachid.ibtiouen@enp.edu.dz,
[2]Laboratoire Plasma et Conversion d'Energie -Unité mixte CNRS-INP Toulouse 2, rue Camichelle - BP 7122- 31071 Toulouse Cedex 7 France. E-mail: maurice.fadel@leei.enseeiht.fr, stephane.caux@leei.enseeiht.fr

The standstill modeling approach has received great emphasis due to its relatively simple testing method where the *d* and *q* axis are decoupled.

Therefore, we present off-line parameters estimation for the synchronous machine. In this work the armature of synchronous machine is respectively fed at standstill by several signals such as PRBS (Pseudo Random Binary Sequences) voltages, PWM voltages and DC decay.

A systematic identification procedure presented in section 3 is used to estimate the parameters of the machine time constant models and equivalent circuit models directly from the time response data. [5-6]

We estimate experimental data with analysis expressions, which contain machine parameters dedicated by a computer program. In the frequency and time-domain analysis, there is a non-linear problem difficult to solve due to the difficulty of linearizing the problem, our approach is based on Levenberg-Marquardt algorithm. In this present research work system identification model concepts and standstill frequency data are used to identify parameters of synchronous machine with the following specifications: $1.5\,\text{kVA}$, $380\,\text{V}$, and $1500\,\text{rpm}$.

2 Synchronous Machine Modeling

For synchronous machine studies, two-axis equivalent circuits with two or three damping windings are usually assumed at the proper structures [6]. Using the Park's d and q-axis reference frame, the synchronous machine is supposed to be modeled with one damper winding for the d-axis and two windings for the q-axis (2×2 model) as shown in Fig. 1 [6-10].

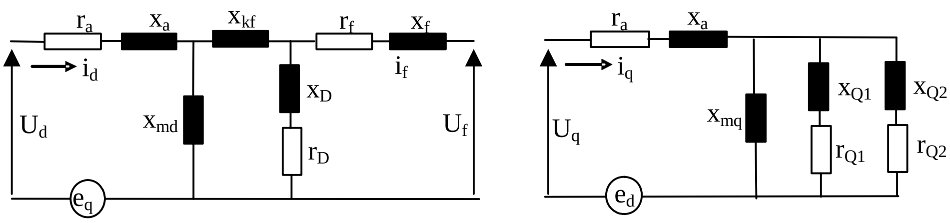

Fig. 1 – *Standard d-q axis circuit models.*

2.1 Voltage equations

$$V_d(p) = r_a i_d(p) + p\varphi_d(p) - \omega_r \varphi_q(p), \tag{1.a}$$

$$V_q(p) = r_a i_q(p) + p\varphi_q(p) + \omega_r \varphi_d(p), \tag{1.b}$$

$$V_f(p) = r_f i_f(p) + p\varphi_f(p), \quad (1.c)$$

$$0 = r_D i_D(p) + p\varphi_D(p), \quad (1.d)$$

$$0 = r_Q i_Q(p) + p\varphi_Q(p). \quad (1.e)$$

While eliminating φ_f, i_f, φ_D, i_D, φ_Q, i_Q we obtains the following equations:

$$V_d(p) = r_a i_d(p) + p\varphi_d(p) - \omega_r \varphi_q(p), \quad (2.a)$$

$$V_q(p) = r_a i_q(p) + p\varphi_q(p) + \omega_r \varphi_d(p), \quad (2.b)$$

$$\varphi_d(p) = X_d(p) i_d(p) + G(p) V_f(p), \quad (2.c)$$

$$\varphi_q(p) = X_q(p) i_q(p). \quad (2.d)$$

This writing form of the equations has the advantage of being independent of the number of damper windings considered on each axis.

In fact, it is the order of the functions $X_d(p)$, $X_q(p)$ and $G(p)$, which depend on the number of dampers.

2.2 Reduced models order

In theory we can represent a synchronous machine by an unlimited stator and rotor circuits. However, the experience show, in modeling and identification there is seven models structures which can be used. The complex model is the 3x3 model which have a field winding, two damper windings on the direct axis, and three on the quadrature axis.

The more common representation is the one deduced from the second order characteristic equation which describes the 2x2 model [8-10]

Damper circuits, especially those in the quadrature axis provide much of the damper torque. This particularity is important in studies of small signal stability, where conditions are examined about some operating point [10]. The second order direct axis models includes a differential leakage reactance. In certain situations for second order models, the identity of the transients field winding. Alternatively, the field circuit topology can alter by the presence of an excitation system, with its associated non-linear features.

For machine at standstill, the rotor speed is zero $(\omega = 0)$ and using the p Laplace's operator, the voltage equations are:

- For the d -axis

$$V_d = \left[r_a + \frac{P}{\omega_0} X_d(p) \right] i_d + pG(p) v_f \,, \tag{3.a}$$

$$V_f = \left[r_f + \frac{p}{\omega_0} X_f(p) \right] i_f + \frac{p}{\omega_0} X_{md} i_d \,. \tag{3.b}$$

- For the q -axis

$$V_q = \left[r_a + \frac{p}{\omega_0} X_q(p) \right] i_q \,. \tag{3.c}$$

With the operational reactances are:

$$X_{d,q,f}(p) = X_{d,q,f} \, \frac{(1+pT'_{d,q,f})(1+pT''_{d,q,f})}{(1+pT'_{d0,q0,f0})(1+pT''_{d0,q0,f0})} \,. \tag{4.a}$$

And the operational function $G(p)$ is:

$$G(p) = \frac{X_{md}}{r_f} \frac{1}{1+pT'_{d0}} \,, \tag{4.b}$$

where d , q , f denote the d -axis, q -axis and field respectively. From these equations it follows that only the three functions $X_d(p)$, $X_q(p)$ and $G(p)$ are necessary to identify a synchronous machine. In the original theory, the quadrature axis has no transient quantities. However, the DC measurements at standstill recommended by IEC, and also the short-circuit tests in the quadrature axis show that the real machine also has transient values $X'_q(p)$, T'_q in addition to the sub transient values $X'_q(p)$, T''_q .

In this study, voltage is the input signal and current is the output signal. Therefore, the transfer functions are in the form of admittances.

The reduced operational admittances of *d*-axis and *q*-axis are reduced from the input-output signals

$$Y_{d,q}(p) = \frac{i_{d,q}(p)}{V_{d,q}(p)} \,.$$

Or in other terms:

$$Y_{d,q}(p) = \frac{1 + p(T'_{d0,q0} + T''_{d0,q0}) + p^2 T'_{d0,q0} T''_{d0,q0}}{r_a + p(r_a(T'_{d0,q0} + T''_{d0}) + \frac{x_{d,q}}{\omega_0}) + p^2(r_a T'_{d0} T''_{d0} + \frac{x_{d,q}}{\omega_0}(T'_{d,q} + T''_{d,q}) + p^3 \frac{x_d}{\omega_0} T'_{d,q} T''_{d,q}} .$$

The reduced operational admittances take the following forms

$$H_{d,q}(p) = \frac{b_0 + b_1 p + b_2 p^2}{1 + a_1 p + a_2 p^2 + a_3 p^3} . \quad (5.a)$$

The synchronous machine parameters are identified by:

$$b_0 = \frac{1}{r_a} , \quad (5.b)$$

$$b_1 = \frac{T'_{d0,q0} + T''_{d0,q0}}{r_a} , \quad (5.c)$$

$$b_2 = \frac{T'_{d0,q0} T''_{d0,q0}}{r_a} , \quad (5.d)$$

$$a_1 = T'_{d0,q0} + T''_{d0,q0} + \frac{x_{d,q}}{\omega_0 r_a} , \quad (5.e)$$

$$a_2 = \frac{x_{d,q}}{\omega_0 r_a}(T'_{d,q} + T''_{d,q}) + T'_{d0,q0} T''_{d0,q0} , \quad (5.f)$$

$$a_3 = \frac{x_{d,q}}{\omega_0 r_a} T'_{d,q} T''_{d,q} . \quad (5.g)$$

Equations (5.a-5.g) show that to determine the various parameters and time-constants of the machine, we have to calculate the constant values a_1, a_2, a_3, b_0, b_1 and b_2 by using the non-linear programming method. For this reason we have used a program, which makes it possible to compute from the input-output signals for each axis (see Figs. 3-6), the parameters quoted above. The model structure selected, which means that the form of the transfer function is known. The numerator order and the denominator one are respectively: Num=2 and Den=3.

The objective of our identification task is to compare the simulated model response and the actual response by minimizing the error between them. For minimizing this error, a good optimization technique is needed. For that we used a quadratic criterion to quantify the difference between the process and the model. Our approach is based on Levenberg-Marquardt algorithm.

3 Identification of Synchronous Machine Parameters

3.1 Time domain tests

In this section, the practical aspects of measurements are described and machine conditions for standstill tests are also given [6-10].The tests are described in IEC34-4A and ANSI-IEEE Std.115A publications [2-3]. It is very easy to perform in practice. PRBS voltage, PWM voltage and DC voltage are applied to two terminals of the three-phase stator windings at standstill.

The alignment of the rotor can be accomplished with shorted excitation winding. A sine wave voltage is applied between two phases of the stator. The duration of the voltage application should be limited to avoid serious over-heating of solid parts. The rotor is slowly rotated to find the angular positions corresponding to the maximum value of the excitation current that gives the direct axis and zero value of the excitation winding current that corresponds to the quadrature axis. This procedure is used by the authors [2, 5, and 6]. Fig. 2 shows the experimental procedure of identification.

The machine is not saturated during standstill tests; in fact, the flux densities are below those on the more linear part of the permeability characteristic that is commonly referred to as “unsaturated”. The determination of quantities referred to the unsaturated state of the machine must be done from tests, which supply voltages (1 to 2%) of the nominal values.

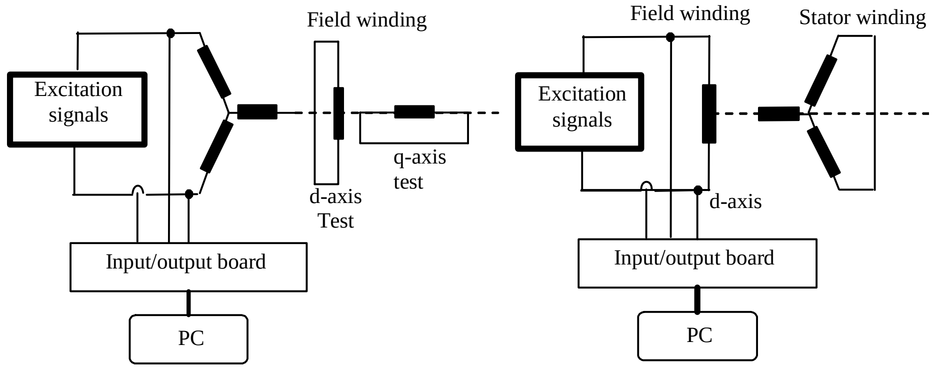

Fig. 2 – *Experimental procedure of identification.*

3.1.1 Experimental procedure.

The two principal characteristic parameters, which relate to the definitions listed, are:

$Z_d(p)$: the direct-axis operational impedance equal to $r_a + pl_q(p)$, where r_a is the DC armature resistance per phase and

$Z_q(p)$: the quadrature-axis operational impedance equal to $r_a + pl_q(p)$.

The above two quantities are the stator driving point impedances. An alternative method of measuring this parameter is presented as fellows:

$$G(p) = \frac{I_{fd}(p)}{pI_d(p)} \text{ for } E_{fd} = 0 . \tag{6}$$

With a shorted field winding $(V_f = 0)$, the d-and q-axis operational admittances are given:

$$Y_{d,q}(p) = \frac{i_{d,q}(p)}{v_{d,q}(p)} \text{ for } V_f = 0 . \tag{7}$$

With a d-axis armature shorted ($V_d = 0$), the field winding parameters can be obtained by:

$$Y_f(p) = \frac{i_f(p)}{v_f(p)} \text{ for } V_d = 0 . \tag{8}$$

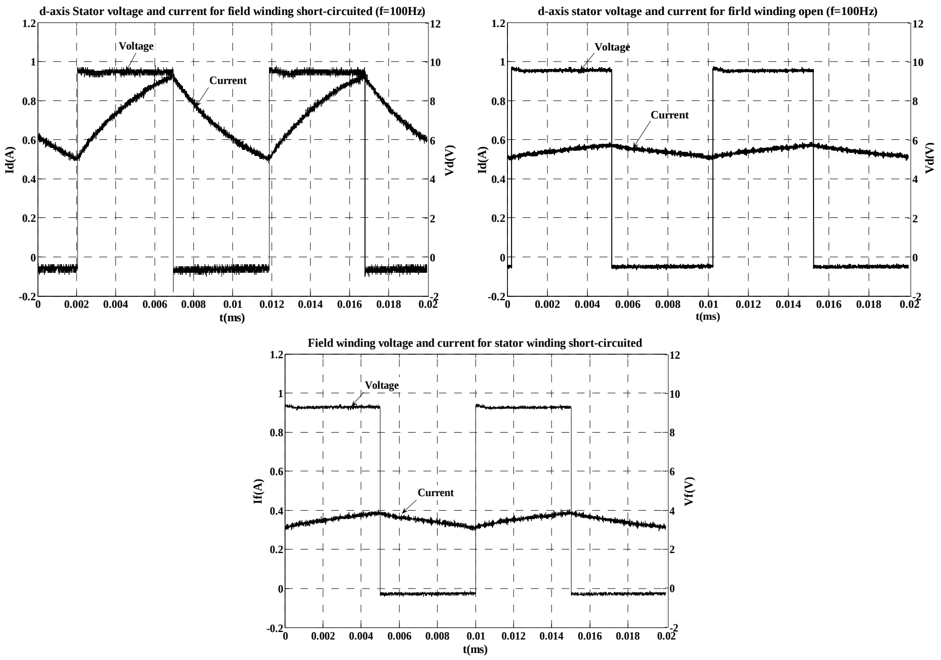

Fig. 3 – *Windings excited by a DC - Chopper.*

Some experimental input-output data, stator voltages and currents, for open and short-circuited field winding, and field winding voltages and currents, are presented in (Figs. 3 - 6). It should be noted that the figures presented correspond to the d -axis; similar curves were measured for the q -axis.

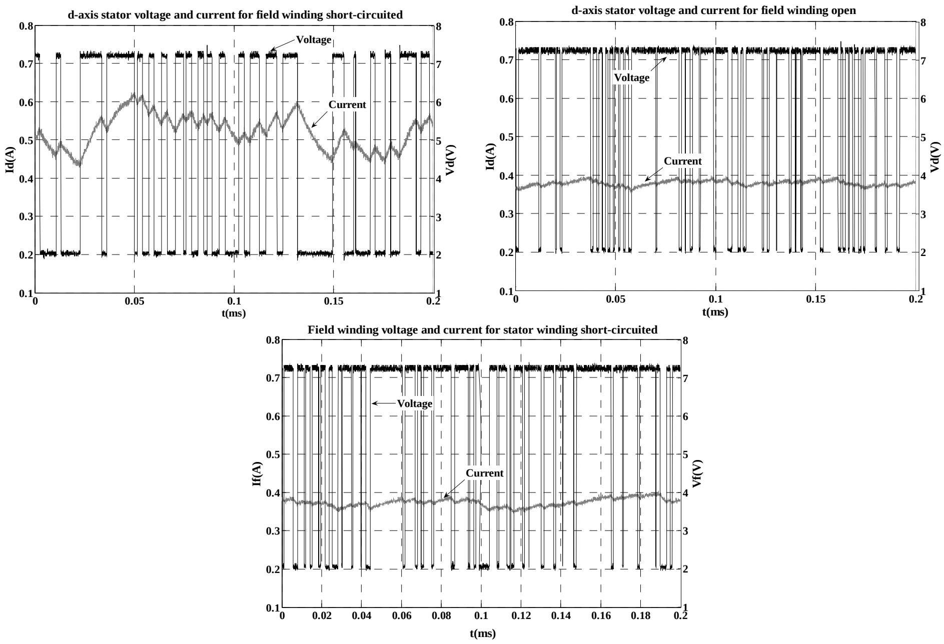

Fig. 4 – *Windings excited by PRBS voltages.*

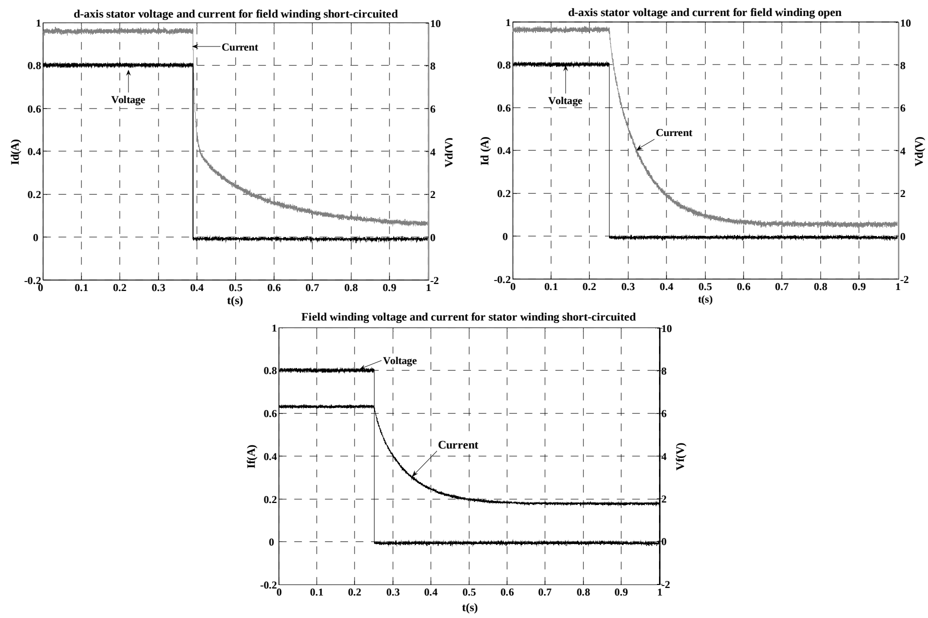

Fig. 5 – *Windings excited by a DC voltage.*

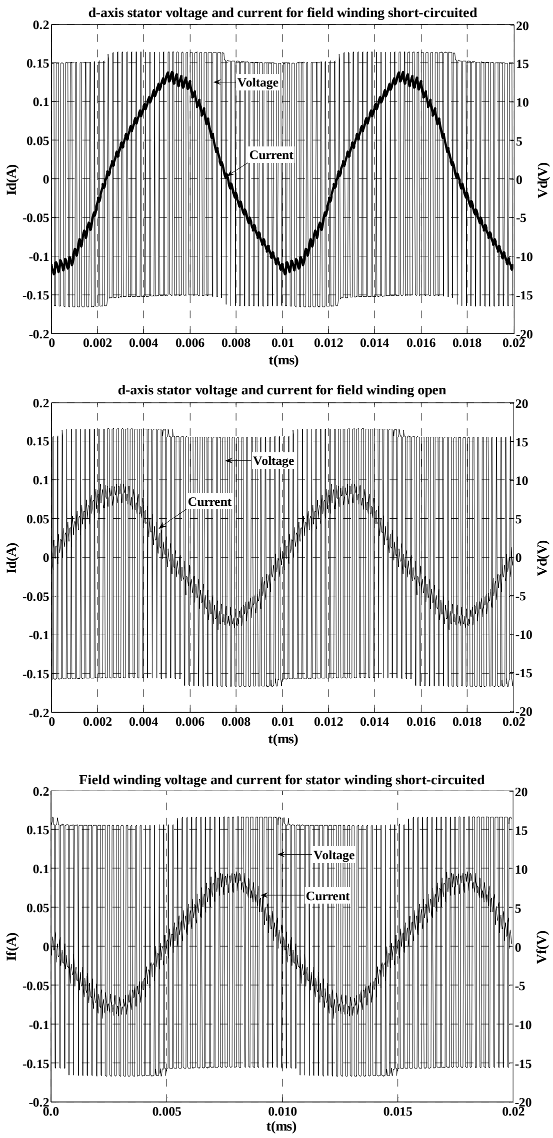

Fig. 6 – *Windings excited by PWM voltages.*

3.2 Frequency response tests

Many papers have been published on the modeling and parameter estimation of synchronous machines using the standstill frequency response test data [3, 11, 12]. Frequency response data describe the response of machine fluxes to stator current and field voltage changes in both the direct and quadrature axes of a synchronous machine. Some advantages of the method are that it can be done either in the factory or on site, it poses a low probability of risk to the machine being tested, and it provides complete data in both direct and quadrature axes.

The tests procedure and the measuring circuits are detailed in reference [3].

3.2.1 Test procedure

The procedure for determining the values of synchronous machine parameters, using the frequency response tests data, follows several steps:

Step 1 is the standstill frequency response process; it determines the data of operational impedances and transfer functions, which punitively describe the interactions of voltages and currents as functions of frequency.

Step 2 is the determination of transfer functions to quantize the current-flux-voltage relations in simple, standard forms, such as $X_d(P)$. Step 2 is a conventional curve fitting process.

Step 3 is the determination of equivalent circuit data (r_j, X_i, T_i, etc.) That is used in simulations from the transfer functions of step 2.

The magnitude and phase of the desired quantities $Z_d(p), Z_q(p)$ and $\frac{\Delta i_{fd}(p)}{\Delta i_q(p)}$ are measured over a range of frequencies.

3.2.2 Measurable parameters at standstill

According to the various test setups, the tests that we have realized correspond to the following equations:

$$Z_d(p) = -\left.\frac{\Delta e_d(p)}{\Delta i_d(p)}\right|_{\Delta e_{fd}=0}, \tag{9.a}$$

$$Z_q(p) = -\frac{\Delta e_q(p)}{\Delta i_q(p)}, \tag{9.b}$$

$$G(p) = \left.\frac{\Delta e_d(p)}{p\Delta e_{fd}(p)}\right|_{\Delta i_d=0}. \tag{9.c}$$

An alternative method of measuring this parameter is suggested as follows:

$$pG(p) = \left.\frac{\Delta i_{fd}(p)}{\Delta i_d(p)}\right|_{\Delta e_{fd}=0}. \tag{9.d}$$

The advantage of the latter form is that it can be measured at the same time as $Z_d(p)$. A fourth measurable parameter at standstill is the armature to field transfer impedance:

$$Z_{af0}(p) = -\frac{\Delta e_{fd}(p)}{\Delta i_d(p)}\bigg|_{\Delta i_{fd}=0} . \tag{9.e}$$

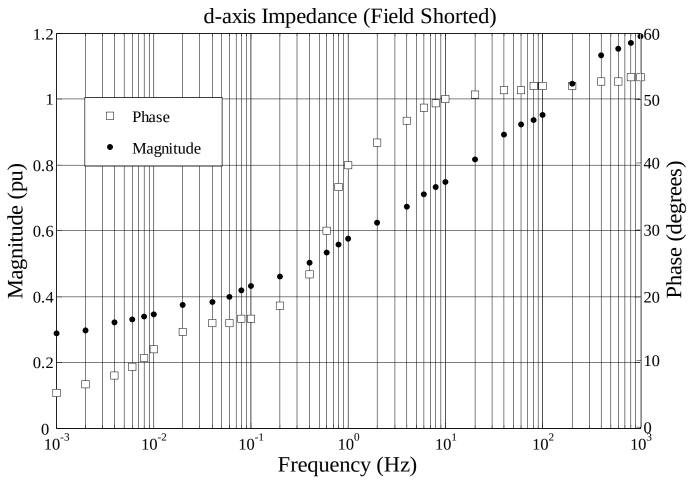

Fig. 7 – *d-axis impedance.*

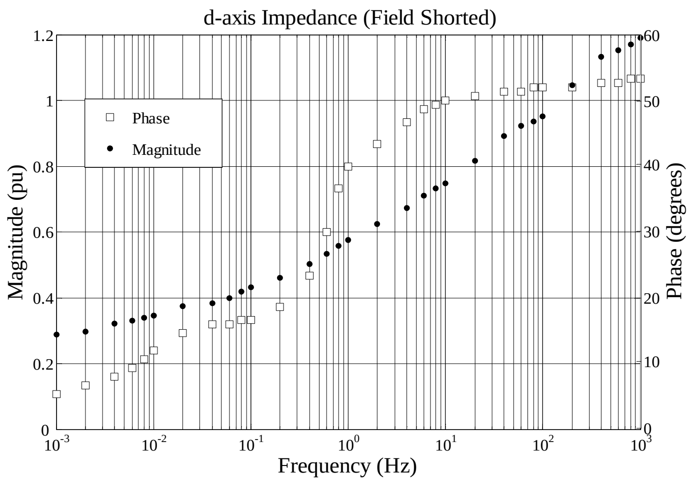

Fig. 8 – *q-axis impedance.*

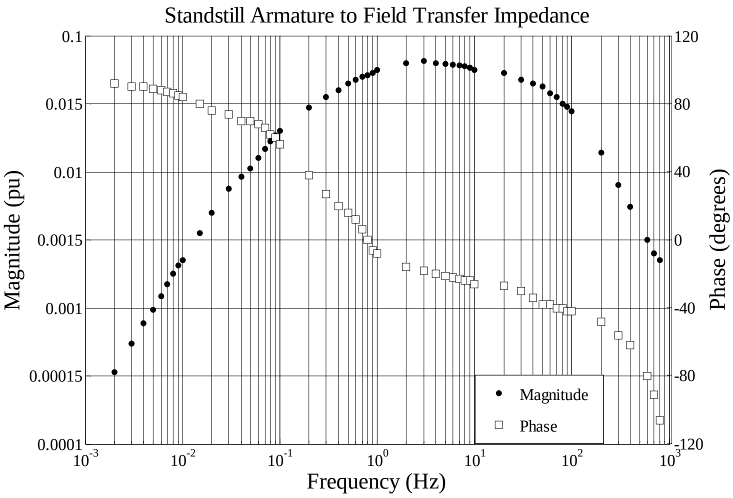

Fig. 9 – *Standstill Armature to Field Transfer Impedance.*

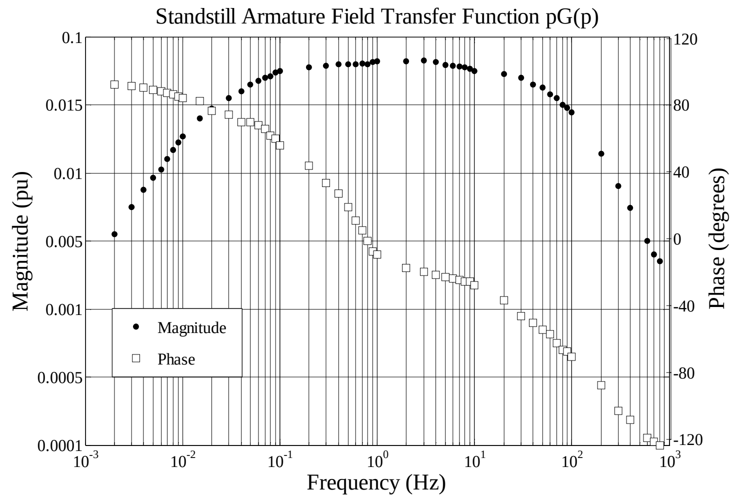

Fig. 10 – *Standstill Armature Field Transfer Function pG(p).*

The relationships between the measured quantities and desired variables are given by:

- d - axis parameters

$$L_d(p) = \frac{Z_d(p) - r_a}{p}, \tag{10.a}$$

$$Z_d(p) = \frac{1}{2} Z_{armd}(p) \text{ and } R_z = \frac{1}{2}\left[\lim_{s \to 0} \left| Z_{armd}(p) \right| \right]. \tag{10.b}$$

To obtain R_a, we plot the real component of this impedance as a function of frequency, and we extrapolate it to zero frequency to get the dc resistance of the two phases of the armature winding in series.

Then we calculate $pG(p)$ by:

$$\frac{\Delta i_{fd}(p)}{\Delta i_d(p)} = \frac{\sqrt{3}\Delta i_{fd}(p)}{2\Delta i\ (p)}. \tag{10.c}$$

Finally, we measure the ratio $\frac{\Delta e_{fd}}{\Delta i}$, and we calculate

$$Z_{af0}(p) = \frac{\Delta e_{fd}(p)}{\Delta i_d(p)} = \frac{\sqrt{3}}{2}\left(\frac{\Delta e_{fd}(p)}{\Delta i(p)}\right), \tag{10.d}$$

- q-axis parameters

$$L_q(p) = \frac{Z_q(p) - r_a}{p}, \tag{11.a}$$

$$Z_q(p) = \frac{1}{2} Z_{armq}(p) \text{ and } r_z = \frac{1}{2}\left[\lim_{s\to 0}\left|Z_{armq}(p)\right|\right]. \tag{11.b}$$

Fig. 11 represents the direct axis operational inductances for each frequency at which $Z_d(p)$ was measured.

The quadrature-axis operational reactance, $X_q(p)$, plotted in Fig. 12, is obtained in the same way from $Z_d(p)$.

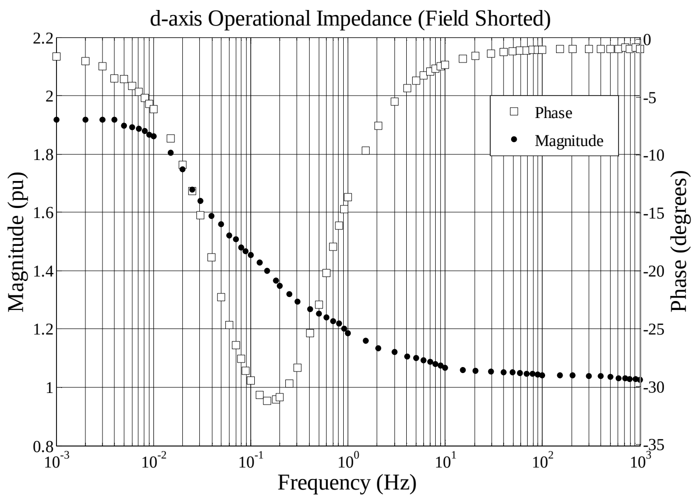

Fig. 11 – *d-axis Operational Impedance.*

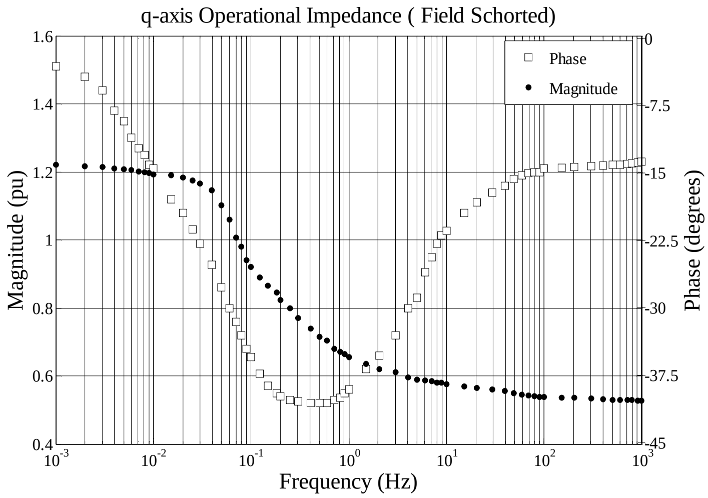

Fig. 12 – *q-axis Operational Impedance.*

3.2 Experimental results

Table 1 and Table 2 presents the parameter values of a synchronous machine from tests using in this study.

Table 1

Synchronous Machine Parameter Values
Identified by Four Excitation Signals.

Parameters	DC-chopper voltages (f =100Hz)	PRBS voltages	DC decay	PWM voltages (f =100 Hz)	Frequency response tests
$r_a\,(p.u)$	0.149	0.149	0.149	0.149	0.15
$r_f\,(p.u)$	4.95	4.95	4.95	4.95	4.942
$T_d'\,(s)$	0.1846	0.1675	0.1840	0.2045	0.1842
$T_d''\,(s)$	0.0486	0.0526	-	0.0471	0.0475
$T_{d0}'\,(s)$	1.1107	0.9189	1.1346	1.1943	1.0706
$T_{d0}''\,(s)$	0.4758	0.4785	-	0.5060	0.4290
$T_q'\,(s)$	0.1498	0.1284	0.1509	0.1782	0.1450
$T_q''\,(s)$	0.0415	0.0361	-	0.0432	0.0390
$T_{q0}'\,(s)$	0.9822	0.7849	1.0279	1.0360	0.8995
$T_{q0}''\,(s)$	0.4035	0.3829	-	0.4348	0.4520
$T_f'\,(s)$	0.2205	0.2306	0.2185	0.2271	-

Table 2
Synchronous Machine Parameter Values
Identified by Four Excitation Signals.

Parameters	DC-chopper voltages (f =100Hz)	PRBS voltages	DC decay	PWM voltages (f =100 Hz)	Frequency response tests
$X_f\ (p.u)$	0.5314	0.5438	0.5287	0.5386	-
$X_d\ (p.u)$	2.0577	1.9980	2.0515	1.9314	1.9850
$X'_d\ (p.u)$	0.3656	0.3459	0.3758	0.3857	0.3450
$X_q\ (p.u)$	1.3685	1.5639	1.3880	1.6328	1.3825
$X'_q\ (p.u)$	0.2267	0.1904	0.2413	0.2158	0.2130
$X''_d\ (p.u)$	0.0368	0.0345	-	0.0343	0.380
$X''_q\ (p.u)$	0.0208	0.0198	-	0.0209	0.203

The frequency and time domain approach offers a methods, which can yield useful models, particularly if the data, are correctly treated.

Taking into account the difficulties associated to the classical test analysis, the identification of synchronous machine is more and more oriented to the static tests. Nevertheless, the choice of supply signals is very important as the choice of model.

The proposed model, the quality and the experimental data used to identify the model parameters and the robustness of the estimation technique, affects the fidelity of synchronous machine models. It is well known that the synchronous machine has a highly complex structure. However, under practical consideration, such complexity has been redefined and reduced following the intended application [6].

3.3 Model validation

The identified $d-q$ axis models are verified by comparing their simulated $d-q$ axis stator currents responses against the measured standstill response, for that we present in Figs. 13-16, simulation results for d and q-axis stator current for signals among those presented previously.

The measured and simulated responses to off-line excitation disturbances comparison show that the machine linear parameters are accurately estimated to represent the machine at standstill conditions.

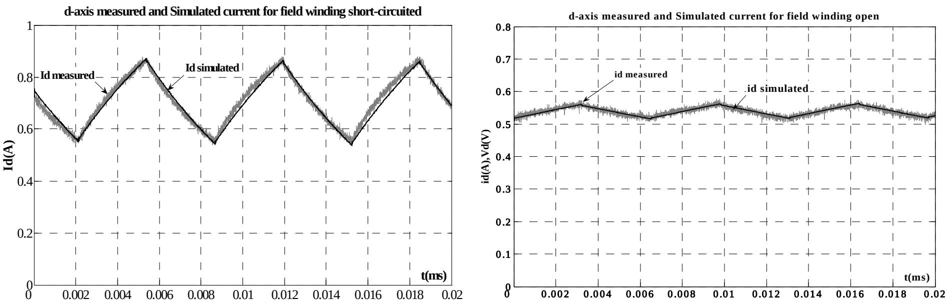

Fig. 13 – *Comparison between real data output and simulated data output, armature current for field winding open and short circuited (DC-chopper voltages) respectively.*

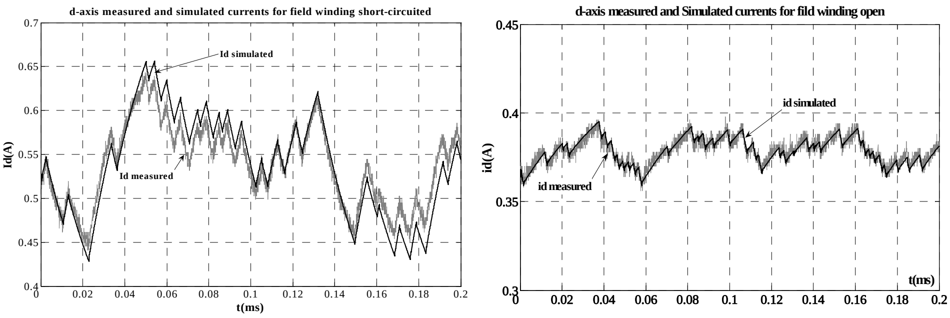

Fig. 14 – *Comparison between real data output and simulated data output, armature current for field winding open and short circuited (PRBS voltages) respectively.*

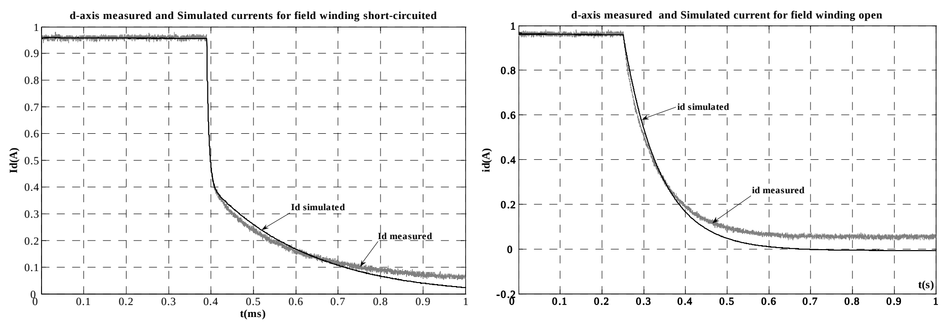

Fig. 15 – *Comparison between real data output and simulated data output, armature current for field winding open and short circuited (DC decay) respectively.*

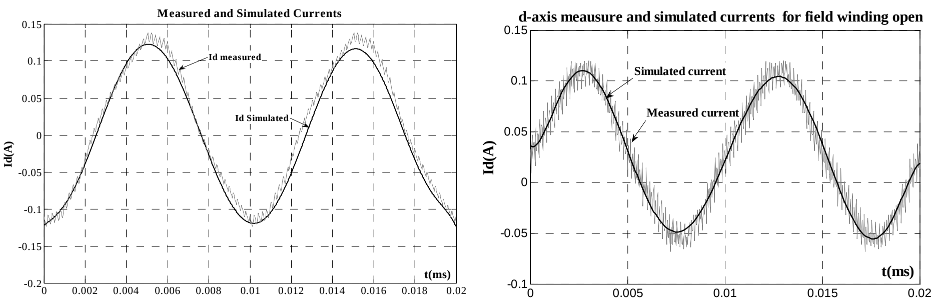

Fig. 16 – *Comparison between real data output and simulated data output, armature current for field winding open and short circuited (PWM voltages) respectively*.

List of Symbols

p	Laplace's operator
ω, ω_0	angular speeds
X_f	field leakage reactance
X_d , X_q	d - and q -axis synchronous reactances
X_{md} , X_{mq}	d - and q -axis magnetizing reactances
r_{Q1}	q -axis damper leakage reactance
X_{Q1} , X_{Q2}	q -axis damper resistances
r_{Q1} , r_{Q2}	d - and q -axis operational admittances
$Y_{d,q}(p)$	d -axis transient open circuit and short-circuit time constant
T_d' , T_{d0}'	q -axis transient open circuit and short-circuit time constant
T_q' , T_{q0}'	d -axis subtransient open circuit and short-circuit time constant
T_d'' , T_{d0}''	q -axis subtransient open circuit and short-circuit time constant
T_q'' , T_{q0}''	armature and field resistances
r_a , r_f	d - and q -axis stator voltages
V_d , V_q	d - and q -axis stator currents
i_d , i_q	d -axis field voltage and current

4 Conclusion

This paper presents a step-by-step procedure to identify the parameter values of the $d-q$ axis synchronous machine models using the standstill time-domain data analysis.

A three-phase salient-pole laboratory machine rated $1.5\,\mathrm{kVA}$ and $380\,\mathrm{V}$ is tested at standstill and its parameters are estimated. Both the transfer function model and the equivalent circuit model parameters are identified using the Levenberg-Marquardt algorithm.

The standstill test concept is preferred because there is no interaction between the direct and the quadrature axis, and it can be concluded that the parameter identification for both axis may be carried out separately. This tests method had been used successfully on our synchronous machine at standstill and gave all the Parks model parameters. Among the advantages claimed for the time and frequency-domain approach at standstill is that the tests are safe and relatively inexpensive.

It should be noted that the various signals used made it possible to determine all the parameters of the equivalent circuits, except for the dc decay test which does not enable us to determine the parameters varying very fast. The identified parameters are in agreement for different tests signals. Furthermore, information's about the quadrature axis, as well as the direct axis of the machine are obtained. The validation of the estimated synchronous machine model parameters is performed by direct comparisons between the measured and simulated standstill time domain responses. The results show that the machine linear parameters are accurately estimated to represent the machine standstill condition.

5 References

[1] E.C. Bortoni, J.A. Jardini: A Standstill Frequency Response Method for Large Salient Pole Synchronous Machines, IEEE Trans on E.C, Vol 19, No. 4, December 2004, pp. 687-691.

[2] IEC Recommendations for Rotating Electrical Machinery, Part.4: Methods for Determining Synchronous Machine Quantities, IEC, 34-4A. 1985

[3] IEEE Guide: Test Procedures for Synchronous Machines, IEEE Std. 115-1995.

[4] H. Guesbaoui, C. Iung and O. Touhami: Towards Real Time Parameter Identification Methodology for Electrical Machine, IEEE-PES Stockholm Tech. Conf, 1995, pp. 91-96.

[5] S. Horning, A. Keyhani, I. Kamwa,: On-line Evaluation of Round Rotor Synchronous Machine Parameter Set Estimation from Standstill Time-domain Data, IEEE Trans on E.C, Vol 12, No. 4, December 1997.

[6] M. Hasni, O Touhami, R Ibtiouen, M. Fadel: Modelling and Identification of A Synchronous Machine by Using Singular Perturbations. IREE, Aug 2006, pp. 418-425.

[7] O. Touhami, H. Guesbaoui, C. Iung: Synchronous Machine Parameter Identification Multitime Scale Technique. IEEE Trans. On Ind. Ap. Vol. 30, No. 5, 1994, pp 1600- 1608.

[8] N. Dedene, R. Pintelon and P. Lataire: Estimation of a Global Synchronous Machine Model using A Multiple Input Multiple Output Estimators, IEEE Trans. On E.C., Vol. 18, No. 1, Feb.2003, pp. 11-16.

[9] V. Graza, M. Biriescu, Gh. Liuba, V. Cretu: Experimental Determination of Synchronous Machines Reactances from DC Decay at Standstill: IEEE Instrumentation and measurement technology conference, Budapest, Hungary, May 2001, pp. 1954-1957.

[10] H. Bora Karayaka, A. Keyhani, B. Agrawal, D. A Selin and G T Heydt: Identification of Armature, Field, and Saturated Parameters of Large Steam Turbine-Generator From Operating Data, IEEE Trans. on E.C., Vol 15, No. 2, June 2000, pp. 181-187.

[11] I. Kamwa, P. Viarouge, H. Le-Huy, J. Dickinson: A Frequency-Domain Maximum Likelhood Estimation of Synchronous Machine High-Order Models Using SSFR Test Data, IEEE Trans. on E.C., Vol. 7, No. 3, September 1992, pp. 525-536.

[12] I. M. Canay: Determination of the Model Parameters of Machines from the Reactance Operators xd(p), xq(p) (Evaluation of SSFR), IEEE Trans. on E.C., Vol. 8, No. 2, June 1993, pp. 272-279.